

Various Magnetic Properties of M -doped CoSb_3 ($M = \text{Sc}, \text{Ti}, \text{V}$, and Mn) Thin Films

Kazuaki KOBAYASHI^{1*}, Masato SHIMONO¹, and Takao MORI^{1,2}

¹*Research Center for Materials Nanoarchitectonics (MANA), National Institute for Materials Science, Namiki 1-1, Tsukuba, Ibaraki 305-0044, Japan*

²*Graduate School of Pure and Applied Sciences, University of Tsukuba, 1-1-1 Tennodai, Tsukuba, Ibaraki 305-8671, Japan*

M -doped CoSb_3 and related compound thin films ($M = \text{Sc}, \text{Ti}, \text{V}$, and Mn) have been calculated in order to investigate their electronic and magnetic properties by using the total energy calculation method. All calculated thin films are free-standing in the supercell and their internal structures are fully relaxed. A vacuum region and slab as a thin film were periodically repeated in the supercell. We considered symmetric and unusual slab structures. Various dopants ($\text{Sc}, \text{Ti}, \text{V}$, and Mn) are considered in order to search novel electronic and magnetic properties and to compare them with each other. We have found various magnetic properties. Although V and Mn dopants have large magnetic moments, those of Sc and Ti dopants are quite small with the exception of one Ti doped case. One of the magnetic states in the Ti -doped unusual thin films is antiferromagnetic. As a result of calculations, total magnetic moments of thin films and the magnetic moment of Mn dopant are enhanced in the unusual thin film case. Most thin films calculated in the present work have ferromagnetic properties. The total energies of the ferromagnetic thin films are lower than those of the nonmagnetic thin films with the exception of Sc - and Ti -doped cases. The magnetic properties generated by the dopants depend on their atomic kinds and positions.

*KOBAYASHI.Kazuaki@nims.go.jp

1. Introduction

CoSb₃ (bulk) is a famous skutterudite compound and its thin films have been investigated both theoretically and experimentally.^{1–11)} Bulk CoSb₃ (Im $\bar{3}$ crystal symmetry) is a semiconductor and its magnetic property is nonmagnetic. In the previous work, Si- and Te-doped CoSb₃ (skutterudite) compounds under high pressure⁹⁾ and Cr-doped CoSb₃ thin films¹⁰⁾ have been extensively investigated in detail. In addition to above studies, a large number of experimental and theoretical studies^{12–37)} of CoSb₃ bulk and thin films have been devoted to elucidate and control their electronic properties. CoSb₃ thin films have been studied for potential and useful thermoelectric materials.^{13, 15, 19–28, 30–33, 36)} Furthermore, the electronic states of CoSb₃ thin films^{12–28, 30–33, 36)} are nonmagnetic. Therefore, there is a general lack of studies on magnetic CoSb₃ thin films.

We focus on the CoSb₃ thin films with transition metal dopants in this work. A thin film is one of the typical nanostructures. It is expected to realize novel electronic and magnetic properties of transition metal atom doped CoSb₃ thin films to enhance the thermoelectric properties. *M*-doped CoSb₃ and related compound thin films (*M* = Sc, Ti, V, and Mn) have been considered and their electronic, lattice, and magnetic properties were obtained and investigated vigorously in this work. Previously, we have already studied the magnetic properties of Cr-doped CoSb₃ thin films.¹⁰⁾ The purpose of this work is to find the new and novel feature of electronic and magnetic properties of CoSb₃ thin films with dopants (Sc, Ti, V, and Mn). These dopants (Sc, Ti, V, Cr,¹⁰⁾ and Mn) have been investigated systematically owing to the various numbers of valence electrons as Sc ($3d^1 4s^2$), Ti ($3d^2 4s^2$), V ($3d^3 4s^2$), Cr¹⁰⁾ ($3d^5 4s^1$), and Mn ($3d^5 4s^2$) to compare their electronic and magnetic properties with each other. We have found various magnetic properties and they are expected to control and tune the electronic properties around the Fermi level. This will lead to enhancing the thermoelectric properties.³⁸⁾

We considered two slab structures as symmetric and unusual in this work. They have been used in the previous work.¹⁰⁾ Total magnetic moments of the “unusual” slab structures are remarkably enhanced. This trend is consistent with the previous results.¹⁰⁾ An analysis of Stoner’s criterion^{39–43)} for magnetic properties of most thin films have been investigated in this work. The total and partial densities of states (TDOSs and PDOSs) at the Fermi level in the nonmagnetic states are fairly important to analyze the stability of magnetic properties using Stoner’s criterion.

2. Calculation Method

Our code^{44, 45)} was used in this work. It is the electronic structure calculation code using the optimized pseudopotential,^{46, 47)} which is based on the local density approximation (LDA) in density functional (DF) theory.^{48, 49)} The exchange-correlation formula by Perdew and Zunger^{50, 51)} was considered. Pseudopotentials^{46, 47)} of Sc, Ti, V, Mn, Co, and Sb were used. Their nonlocal parts were tuned into Kleinman-Bylander separable forms⁵²⁾ without ghost bands. Nonlinear core corrections⁵³⁾ were considered in Sc, Ti, V, and Mn pseudopotentials. The wave functions were expanded in plane waves and the cutoff energy for them was set at 81 Ry. The number of k -points for sampling (N_k) was 16 ($= 4 \times 4 \times 1$) in the whole Brillouin zone. The magnetic moments were obtained from the electron density differences between majority and minority spin states. The TDOSs and PDOSs were obtained from the electronic band structures.⁵⁴⁾ We have assumed a periodically repeated slab model, where slab and vacuum regions were periodically repeated and the slab is free-standing in the supercell. The internal atoms in the slab were governed by Hellmann-Feynman forces.^{55, 56)} These repeated slabs correspond to thin films and their internal atoms were structurally optimized where the maximum force acting on each atom is less than 2.0×10^{-3} Ry/Bohr.

We considered two slab structures in the present work. One is constructed from the crystal structure of bulk skutterudite. The calculated equilibrium lattice constant of bulk CoSb_3 (skutterudite) are 8.953 Å (9.036 Å[Experiment]⁵⁾) and the number of atoms in the primitive unit cell is 16. This slab consists of the cubic unit cell ($= 2$ primitive unit cells) and one Sb layer ($= 4$ atoms) and its number of atoms is 36 (see Fig. 1 (a)). Its composition is $\text{Co}_7\text{M}_1\text{Sb}_{28}$ (M -doped atoms as $M = \text{Sc, Ti, V, and Mn}$) and slab structure is symmetric. The other which corresponds to the related compound was constructed accidentally in the process of constructing the CoSb_3 slab.¹⁰⁾ Its composition as $\text{Co}_7\text{M}_1\text{Sb}_{24}$ (M -doped atoms as $M = \text{Sc, Ti, V, and Mn}$) was considered. Its slab structure is asymmetric and unusual and its atom number in the supercell is 32. Figures 1 (a) and (b) show above two slab structures without dopants in the supercell where some atoms are duplicated due to periodicity in depicting the slab structures hereafter. Co atoms are numbered as shown in Figs. 1 (a) and (b). The M -doped site corresponds to that of the Co atom (“1”). We denote Co atom (“1”) as Co (1), Co atom (“2”) as Co (2), etc. hereafter. These symmetric and unusual slab structures are the same as previous work.¹⁰⁾ We denote these slabs as M -doped CoSb_3 (symmetric) and

M -doped CoSb_3 (unusual) ($M = \text{Sc}, \text{Ti}, \text{V}$, and Mn) hereafter. Cutoff energy, number of k -points, and number of atoms are listed in Table I.

3. Results and Discussion

3.1 Stability

We calculated nonmagnetic (NM) and ferromagnetic (FM) cases where $T = 0$ K in the DFT-LDA calculation. Slab structures in the supercell are fully relaxed. Figures 2 and 3 are bird's eye views of Sc-doped and Ti-doped CoSb_3 (unusual) thin films in nonmagnetic and ferromagnetic states, respectively. Those of Sc- and Ti-doped CoSb_3 (symmetric) thin films in nonmagnetic and ferromagnetic states are shown in Fig. 4. The total energy differences ($\Delta E_{\text{FM-NM}}$) and average atomic position differences per atom ($\Delta D_{\text{FM-NM}}$) between the nonmagnetic and ferromagnetic cases are listed in Table I. Their total magnetic moments are also shown in Table I. $\Delta E_{\text{FM-NM}}$ values of CoSb_3 (symmetric),¹⁰⁾ Sc-doped CoSb_3 (symmetric), and Ti-doped CoSb_3 (symmetric) thin films are fairly small within 0.03 eV. Therefore, their total magnetic moments in the ferromagnetic cases are also small within approximately $0.04 \mu_{\text{B}}$ and they are substantially equal to nonmagnetic. μ_{B} is the Bohr magneton. $\Delta E_{\text{FM-NM}}$ values of the unusual thin films are energetically lower than those of the symmetric thin films. $\Delta D_{\text{FM-NM}}$ values of the unusual thin films are fairly larger than those of the symmetric thin films. Larger $\Delta D_{\text{FM-NM}}$ values lead to more stable slab structures in the ferromagnetic unusual thin films. In unusual cases, ferromagnetic states are more favorable than nonmagnetic states with the exception of Sc doped case. The nonmagnetic Sc-doped CoSb_3 (unusual) thin film is energetically more stable by 3.61 eV than the ferromagnetic case. The relaxed structure of the nonmagnetic Sc-doped CoSb_3 (unusual) thin film is remarkably different from other unusual cases as shown in Figs. 2 (a) and 3 (a). It leads to more stable structure in the relaxation since the unusual thin film has high degrees of structural freedom. This is inconsistent with the relaxed structure of the ferromagnetic Sc-doped CoSb_3 (unusual) thin film. Further consideration is necessary to obtain more suitable relaxed structure of the nonmagnetic Sc-doped CoSb_3 (unusual) thin film.

The relaxed symmetric thin films with dopants are structurally similar to each other as shown in Fig. 4. This trend is consistent with other dopant cases (Ti [see Figs. 4 (c) and (d)], V, and Mn [see Fig. S1 in supplementary data]). Although the relaxed unusual thin films with dopants (Ti, V, and Mn) are also structurally similar to each other, the relaxed structures of nonmagnetic unusual thin films are slightly different

from those of ferromagnetic thin films as shown in Figs. 3 (a) and (b). The evidently different atomic positions between Figs. 3 (a) and (b) are labeled by red numbers and those between Figs. 3 (b) and (c) are labeled by red (1 and 6) and black numbers (11). The $\Delta D_{\text{FM-NM}}$ between Figs. 3 (a) and (b) is 0.571 Å (see Table I) and that of the Ti-doped CoSb₃ (symmetric) thin film is 0.006 Å. The relaxed unusual thin films with dopants (V and Mn) are shown in Fig. S2 (see supplementary data) and evidently different atomic positions between NM and FM cases are labeled by red numbers. These differences are independent of the atomic kind of dopant.

3.2 Magnetic moments

All the calculated thin films in this work are metallic regardless of their magnetic and lattice structures. The total magnetic moments and magnetic moments of dopants (Sc, Ti, V, Cr,¹⁰) and Mn) are shown in Table II. The magnetic moments of V and Mn are large and those of Sc and Ti are fairly small within approximately 0.1 μ_{B} in all cases with the exception of the replaced case. A detailed description of the replaced case will be mentioned in the later. Total magnetic moments of the ferromagnetic unusual thin films are large. The magnetic moments of Cr¹⁰) and Mn dopants are enhanced in the unusual thin film cases from Table II although that of V dopant decreases slightly in the unusual thin film. Although the magnetic moments of V and Mn dopants in the symmetric cases are large, those of Co and Sb are small and less than 0.16 μ_{B} (absolute value).

To confirm these magnetic properties, the magnetic moment of each atom in the V- and Mn-doped CoSb₃ (unusual) thin films is shown in Figs. 5 and 6. From Figs. 5 and 6, the V and Mn dopants in the CoSb₃ (unusual) thin films have large magnetic moments. A dopant is substituted for Co (1) in Co (“1”, “4”, “6”, and “7”) atoms as “lower” (see Fig. 1 and insets of Figs. 5 and 6, see Fig. 3 for numbered Sb atoms). The figures 5 and 6 clearly show that the magnetic moments of V and Mn dopants and Co (“2”, “3”, “5”, and “8”) as “upper” (see Fig. 1) are large. Those of other three Co atoms as “Co (lower)” and Sb atoms are fairly small and negligible in all cases.

The magnetic moments of V, Cr,¹⁰) and Mn dopants in the unusual cases are large although their positions correspond to those of Co (1) and the unusual thin films are energetically quite unfavorable.¹⁰) The magnetic moments of Sc and Ti dopants whose positions correspond to Co (1) are small regardless of their thin film structures. Therefore, we focus on structurally relaxed ferromagnetic Sc- and Ti-doped CoSb₃ (unusual)

thin films as initial structures. We replace the Sc (1) and Ti (1) dopants with Co (2) in ferromagnetic unusual cases to analysis the variation of their magnetic properties as shown in Fig. 1 (c), respectively. The thin film structures with the replacements are structurally relaxed. The magnetic moment of Co (2) is large before replacing. From table II, the magnetic moments of the replaced Co atoms (= Co (1)) without relaxation are large and those are fairly decreased with less than $0.15 \mu_B$ after relaxation. The magnetic moments of the replaced Sc atom with and without relaxation are small with less than $0.1 \mu_B$ (absolute value) as shown in Fig. S3 (see supplementary data). In contrast, the magnetic moments of the replaced Ti atom without and with relaxation are antiferromagnetic and their absolute values are large as shown in Fig. 7 and table II. Therefore, the total magnetic moment of the unusual thin film replaced Ti (1) with Co (2) after structural relaxation is smallest in the unusual thin films. The antiferromagnetic behavior in this work is induced by the Ti dopant. The total energies of unusual thin films with the replacement of Sc (1) - Co (2) and Ti (1) - Co (2) are lower by 0.93 eV and 0.30 eV than those of Sc- and Ti-doped unusual thin films without replacement, respectively. This replacement is almost equal to the substitution of Co (2) for dopant in the CoSb_3 thin film. It is revealed that the magnetic properties of dopants are varied by their atomic kinds and positions. In particular, the magnetic state of the replaced Ti dopant indicates antiferromagnetic behavior. As for magnetic properties, there is a distinctly difference among Sc, Ti, V, Cr,¹⁰⁾ and Mn. Their numbers of valence electrons may play a important role. Therefore, further investigations will be necessary to clarify the mechanism of the antiferromagnetic behavior in the Ti doped case and other various magnetic properties.

3.3 TDOS and PDOS

We calculated the total and partial densities of states (TDOSs and PDOSs) of the structurally relaxed thin films in this work. The TDOSs and PDOSs for the Mn-doped CoSb_3 (symmetric) and (unusual) thin films are plotted in Fig. 8. The TDOSs and PDOSs of Sc- and Ti-doped CoSb_3 (unusual) thin films in nonmagnetic cases are shown in Figs. S4 and S5, respectively (see supplementary data). The TDOSs and PDOSs of Sc-, Ti-, and V-doped CoSb_3 (symmetric) thin films in ferromagnetic cases are shown in Figs. S6, S7, and S8, respectively (see supplementary data). The TDOS and PDOSs of V-doped CoSb_3 (unusual) thin films in the ferromagnetic case are shown in Fig. S9 (see supplementary data). The features of TDOSs and PDOSs in each symmetric (see

Figs. 8 (b), S6, S7, and S8) or unusual (see Figs. 8 (d), 9 (a), 10 (a), and S9) thin film are similar to each other. This is consistent with the similarity between relaxed thin film structures. The PDOS of Mn is remarkably spin polarized in the symmetric case although the PDOSs of Co and Sb are almost unpolarized as shown in Fig. 8 (b). In contrast, the PDOSs of Mn and Co are fairly polarized in the unusual thin film as shown in Fig. 8 (d). These trends are the same for V-doped and Cr-doped¹⁰⁾ CoSb₃ (symmetric) and (unusual) thin films. The TDOSs and PDOSs of Sc- and Ti-doped CoSb₃ (unusual) thin films in ferromagnetic cases are shown in Figs. 9 and 10, respectively. The replacement cases are also plotted in Figs. 9 (b) and 10 (b). The PDOSs of Sc and Ti are almost unpolarized in all cases (see Figs. 9 (a), 9 (b), 10 (a), S6, and S7) with the exception of the replacement of Ti (1) -Co (2). The PDOS of Ti (2) in the thin film with the replacement of Ti (1) - Co (2) is antiferromagnetically polarized in Fig. 10 (b).

The PDOSs of Sb at the Fermi level in the nonmagnetic Mn-doped CoSb₃ (symmetric) thin films are larger than those of Co as shown in Fig. 8 (a) (see inset). In contrast, the contribution of both PDOSs of Co and Sb at the Fermi level in nonmagnetic unusual and ferromagnetic (minority spin) unusual thin films are large and nearly equal to each other as shown in Figs. 8 (c) and (d) (see insets). This trend is consistent with other doped cases (Sc, Ti, V [see Fig. S9], and Cr¹⁰⁾) and inconsistent with the Fe₂VAI thin film cases⁵⁷⁾ where Fe states are dominated at the Fermi level.

3.4 Stoner's criterion

We analyze the stability of the ferromagnetic states using the Stoner's criterion^{39–43)} as a rough estimate. In this criterion, the DOS per spin at the Fermi level ($D(E_f)$) is an important factor. We calculated the $D(E_f)$ values of thin films with dopants (Sc, Ti, V, Cr,¹⁰⁾ Mn, and Co¹⁰⁾) to clarify the stability of the ferromagnetism. We calculated $ID(E_f)$, where I is the exchange parameter,⁴⁰⁾ to determine if Stoner's criterion is satisfied. The $ID(E_f)$ value greater than one ($ID(E_f) > 1$) is favorable for ferromagnetism. We used the values⁴³⁾ of exchange parameters (I , see Table III) of Sc, Ti, V, Cr, Mn, and Co. They are insensitive to the chemical environment⁴¹⁾ because they depend primarily on intra-atom interactions. The calculated $ID(E_f)$ values are tabulated in Table III. The $ID(E_f)$ values of bulk Sc (bcc), Sc (fcc), Sc (hcp), Ti (hcp), V (bcc), Cr (bcc), Mn (fcc), Co (fcc), and Co (hcp) are obtained and most of them are consistent with the calculated magnetic properties with the exception of Co (fcc) and Sc (bcc). The magnetic

states of Sc (bcc) is ferromagnetic although Sc (bcc) is energetically more unfavorable than Sc (fcc) and Sc (hcp). In the previous work,¹⁰⁾ $ID(E_f)$ value of Co (hcp) was 0.9, that is 1.2 in the present work as a result of recalculation. The ferromagnetic states of bulk Sc (fcc), Sc (hcp), Ti (hcp), V (bcc), and Cr (bcc)¹⁰⁾ are unstable and they are consistent with the $ID(E_f)$ value smaller than one.

From Table III, the $ID(E_f)$ values in the nonmagnetic cases are $0.1 \sim 0.7$ and they are smaller than those ($0.8 \sim 1.2$) in the ferromagnetic cases with the exception of the Mn dopant in the symmetric thin film ($ID(E_f) = 0.5$). The smallest $ID(E_f)$ value (0.1) of Sc dopant in the Sc-doped CoSb₃ (unusual) thin film may be invalid because its relaxed structure is quite different from that of the ferromagnetic case as mentioned above. The magnetic moments of V, Cr,¹⁰⁾ and Mn dopants are large and ferromagnetic in all thin film cases. The $ID(E_f)$ values of V, Cr,¹⁰⁾ and Mn dopants (symmetric) and Cr¹⁰⁾ and Mn dopants (unusual), and Sc (bcc) and Co (fcc) bulk in Table III do not satisfy Stoner's criterion. However, their $ID(E_f)$ values ($0.8 \sim 0.9$) are so close to one that they imply ferromagnetic states are stable. This inconsistency leads to beyond the Stoner theory. Some values of Cr, Co, CoSb₃ and Cr-doped CoSb₃, which are listed in Tables I, II, and III, are improved and slightly different from the previous work¹⁰⁾ as the results of recalculation using denser energy meshes for all cases and denser k -point meshes for bulk metals. The differences of recalculations are fairly small within $0.08 \mu_B$ (or within 10 %) in the magnetic moments.

4. Summary

In this work, the electronic and magnetic properties of M -doped CoSb₃ thin films ($M = \text{Sc, Ti, V, and Mn}$) have been calculated. Various magnetic properties have been presented in this work. It is found that the ferromagnetic states for most thin films are energetically more stable. It is revealed that the total magnetic moments of thin films and the magnetic moments of the Mn dopant are enhanced in the unusual thin films. This trend is consistent with previous Cr-doped case.¹⁰⁾ It may be significant to break the symmetry of the thin films for varying the magnetic properties. The magnetic moments of Sc and Ti dopants and Co (lower) and Sb atoms are fairly small with the exception of the Ti (1) - Co (2) replacement case. The replacement of Ti (1) - Co (2) with structural relaxation induces the antiferromagnetic state of Ti dopant although the magnetic moments of Sc in the replacement of Sc (1) - Co (2) with and without relaxation are fairly small. Various magnetic behavior is remarkable and it is expected

to control and tune the electronic and magnetic properties around the Fermi level. In particular, TDOS shapes at the Fermi level are very important for the thermoelectric properties. This will be enhanced the thermoelectric properties.³⁸⁾

The stability of the ferromagnetic states for dopants in the thin films is analyzed using Stoner's criterion³⁹⁻⁴³⁾ as a rough estimate. It is not sufficient to describe the ferromagnetic states using Stoner's criterion although their $ID(E_F)$ values ($0.8 \sim 1.2$) are larger than those ($0.1 \sim 0.7$) in the nonmagnetic cases with the exception of the Mn-doped case. The analysis of Stoner's criterion in this work is possible to describe the magnetic properties qualitatively to a certain extent, whereas it is still insufficient. Therefore, it is necessary to further investigation to clarify the mechanism of the large magnetic moments in the ferromagnetic cases.

More extensive calculations of various slab structures, defects, dopants, co-doping,^{11, 36, 37)} and introducing disorder are needed to tune and enhance the magnetic moments in the thin films. The slabs were terminated by Sb atom layers in all thin films and a layer number of each slab was not varied in the present calculations. Although other asymmetric slab cases have been investigated in the previous work,¹⁰⁾ they are not considered in this work. It is necessary to consider Co-terminated and/or other various thickness of slab cases in order to investigate the stability of the thin films in the future next task.

It is not clear and needs further consideration to the origin of antiferromagnetic behavior of the Ti dopant (Ti (2)) in the Ti (1) - Co (2) replacement case. It is necessary to replace V, Cr, and Mn dopants with Co atoms to investigate and compare with the present results of Sc (1) - Co (2) and Ti (1) - Co (2) replacements. In addition, it is expected that the experimental synthesis and observation of thin films with transition metal dopants calculated in this work will be realized. Their thermoelectric properties (thermal conductivity, Seebeck coefficient, and power factor, etc.) will be obtained theoretically in the future task.

Acknowledgments

This work was supported by the JST-Mirai Program, Grant Number JPMJMI19A1, Japan. The calculations in this work were performed on Z2 workstation (HP) and the numerical materials simulator [HPE SGI 8600] at NIMS. Figures in the present work are depicted by using MATLAB (Mathworks) and Materials Studio (BIOVIA).

References

- 1) D. J. Singh and W. E. Pickett, Phys. Rev. B **50**, 11235 (1994).
- 2) T. Caillat, A. Borshchevsky, and J.-P. Fleurial, J. Appl. Phys. **80**, 4442 (1996).
- 3) J. O. Sofo and G. D. Mahan, Phys. Rev. B **58**, 15620 (1998).
- 4) J. Yang, M. G. Endres, and G. P. Meisner, Phys. Rev. B **66**, 014436 (2002).
- 5) A. C. Kraemer, C. A. Perottoni, and J. A. H. da Jornada, Solid State Commun. **133**, 173 (2005).
- 6) Y. Tang, Z. M. Gibbs, L. A. Agapito, G. Li, H.-S. Kim, M. B. Nardelli, S. Curtarolo, and G. J. Snyder, Nat. Mater. **14**, 1223 (2015).
- 7) M. Rull-Bravo, A. Moure, J. F. Fernández, and M. Martin-González, RSC Adv. **5**, 41653 (2015).
- 8) A. U. Khan, K. Kobayashi, D. Tang, Y. Yamauchi, K. Hasegawa, M. Mitome, Y. Xue, B. Jiang, K. Tsuchiya, D. Golberg, Y. Bando, and T. Mori, Nano Energy **31**, 152 (2017).
- 9) K. Kobayashi, A. U. Khan, and T. Mori, Jpn. J. Appl. Phys. **56**, 05FB07 (2017) and references for CoSb₃ (bulk) therein.
- 10) K. Kobayashi, H. Takaki, M. Shimono, H. Ishii, N. Kobayashi, K. Hirose, and T. Mori, Jpn. J. Appl. Phys. **62**, SC1046 (2023).
- 11) C. Bourgès, W. Zhang, K. K. Raut, Y. Owada, N. Kawamoto, M. Mitome, K. Kobayashi, J.-F. Halet, D. Berthebaud, and T. Mori, ACS Appl. Energy Mater. **6**, 9646 (2023).
- 12) J. C. Caylor, A. M. Stacy, R. Gronsky, and T. Sands, J. Appl. Phys. **89**, 3508 (2001).
- 13) V. Savchuk, A. Boulouz, S. Chakraborty, J. Schumann, and H. Vinzelberg, J. Appl. Phys. **92**, 5319 (2002).
- 14) B. Schüpp, I. Bächer, M. Hecker, N. Mattern, V. Savchuk, and J. Schumann, Thin Solid Films **434**, 75 (2003).
- 15) V. Savchuk, J. Schumann, B. Schüpp, G. Behr, N. Mattern, and D. Souptel, J. Alloys Compd. **351**, 248 (2003).
- 16) A. Dauscher, M. Puyet, B. Lenoir, D. Colceag, and M. Dinescu, Appl. Phys. A **79**, 1465 (2004).
- 17) D. Colceag, A. Dauscher, B. Lenoir, V. D. Ros, R. Birjega, A. Moldovan, and M. Dinescu, Appl. Surf. Sci. **253**, 8097 (2007).

- 18) M. Daniel, M. Friedemann, N. Jöhrmann, A. Liebig, J. Donges, M. Hietschold, G. Beddies, and M. Albrecht, *Phys. Status Solidi A* **210**, 140 (2013).
- 19) G. Fu, L. Zuo, J. Chen, M. Lu, and L. Yu, *J. Appl. Phys.* **117**, 125304 (2015).
- 20) M. V. Daniel, C. Brombacher, G. Beddies, N. Jöhrmann, M. Hietschold, D. C. Johnson, Z. Aabdin, N. Peranio, O. Eibl, and M. Albrecht, *J. Alloys Compd.* **624**, 216 (2015).
- 21) M. V. Daniel, M. Lindorf, and M. Albrecht, *J. Appl. Phys.* **120**, 125306 (2016).
- 22) Z. Zheng, M. Wei, F. Li, J. Luo, G. Liang, H. Ma, X. Zhang, and P. Fan, *Coatings* **7**, 205 (2017).
- 23) M. Bala, S. Gupta, S. K. Srivastava, S. Amrithapandian, T. S. Tripathi, S. K. Tripathi, C.-L. Dong, C.-L. Chen, D. K. Avasthi, and K. Asokan, *Phys. Chem. Chem. Phys.* **19**, 24886 (2017).
- 24) Z. Zheng, F. Li, J. Luo, G. Liang, H. Ma, X. Zhang, and P. Fan, *J. Alloys Compd.* **732**, 958 (2018).
- 25) Z.-H. Zheng, M. Wei, J.-T. Luo, F. Li, G.-X. Liang, Y. Liang, J. Hao, H.-L. Ma, X.-H. Zhang, and P. Fan, *Inorg. Chem. Front.* **5**, 1409 (2018).
- 26) G. Liang, Z. Zheng, F. Li, J. Luo, H. Jin, X. Zhang, and P. Fan, *J. European Ceramic Soc.* **39**, 4842 (2019).
- 27) C. Bourgès, N. Sato, T. Baba, T. Baba, I. Ohkubo, N. Tsujii, and T. Mori, *RSC Adv.* **10**, 21129 (2020).
- 28) A. Kato, C. Bourgès, H. Pang, D. Gutiérrez, T. Sakurai, and T. Mori, *Polymers* **14**, 1986 (2022).
- 29) G. Li, U. Aydemir, M. Wood, W. A. Goddard, III, P. Zhai, Q. Zhang, and G. J. Snyder, *Chem. Mater.* **29**, 3999 (2017).
- 30) A. Ahmed and S. Han, *Appl. Surf. Sci.* **408**, 88 (2017).
- 31) A. Ahmed and S. Han, *J. Alloys Compd.* **790**, 577 (2019).
- 32) K. Yin, L. Shi, Y. Zhong, X. Ma, M. Li, and X. He, *Phys. Chem. Chem. Phys.* **25**, 2517 (2023).
- 33) D. Li, X.-L. Shi, J. Zhu, T. Cao, X. Ma, M. Li, Z. Han, Z. Feng, Y. Chen, J. Wang, W.-D. Liu, H. Zhong, S. Li, and Z.-G. Chen, *Nature Communications* **15**, 4242 (2024).
- 34) A. Saini and U. F. Lone, *Phys. Status Solidi B* **261**, 2300244 (2024).
- 35) Z. L. Guo, Z. L. Liu, X. Wang, and L. Deng, *J. Alloys Compd.* **1002**, 175305 (2024).

- 36) Z.-H. Zheng, J.-Y. Niu, D.-W. Ao, B. Jabar, X.-L. Shi, X.-R. Li, F. Li, G.-X. Liang, Y.-X. Chen, Z.-G. Chen, and P. Fan, *J. Mater. Sci. Technol.* **92**, 178 (2021).
- 37) B. Qin, Y. Ji, Y. Lei, and Y. Li, *Ceramics International* **50**, 28296 (2024).
- 38) G. D. Mahan and J. O. Sofo, *Proc. Natl. Acad. Sci. U.S.A.* **93**, 7436 (1996).
- 39) E. C. Stoner, *Proc. R. Soc. London, Ser. A* **154**, 656 (1936).
- 40) O. Gunnarsson, *J. Phys. F: Metal Phys.* **6**, 587 (1976).
- 41) T. Beuerle, K. Hummler, C. Elsässer, and M. Fähnle, *Phys. Rev. B* **49**, 8802 (1994).
- 42) S. Sakuragi, H. Tajiri, H. Kageshima, and T. Sato, *Phys. Rev. B* **97**, 214421 (2018).
- 43) J. F. Janak, *Phys. Rev. B* **16**, 255 (1977).
- 44) K. Kobayashi, The electronic properties and optimized structures of the alkali adsorbed Si(001) surface by using the first principles molecular dynamics, PhD thesis (Univ. of Tokyo), 1991.
- 45) K. Kobayashi, Y. Morikawa, K. Terakura, and S. Blügel, *Phys. Rev. B* **45**, 3469 (1992).
- 46) N. Troullier and J. L. Martins, *Phys. Rev. B* **43**, 1993 (1991).
- 47) K. Kobayashi, *Mater. Trans.* **42**, 2153 (2001).
- 48) P. Hohenberg and W. Kohn, *Phys. Rev.* **136**, B864 (1964).
- 49) W. Kohn and L. J. Sham, *Phys. Rev.* **140**, A1133 (1965).
- 50) D. M. Ceperley and B. J. Alder, *Phys. Rev. Lett.* **45**, 566 (1980).
- 51) J. Perdew and A. Zunger, *Phys. Rev. B* **23**, 5048 (1981).
- 52) L. Kleinman and D. M. Bylander, *Phys. Rev. Lett.* **48**, 1425 (1982).
- 53) S. G. Louie, S. Froyen, and M. L. Cohen, *Phys. Rev. B* **26**, 1738 (1982).
- 54) S. G. Louie and M. L. Cohen, *Phys. Rev. B* **10**, 3237 (1974), see the section II.B.
- 55) H. Hellmann. *Einführung in die Quanten Theorie.* (Deuticke, Leipzig), 1937.
- 56) R. P. Feynman. *Phys. Rev.* **56**, 340 (1939).
- 57) K. Kobayashi, H. Takaki, M. Shimono, H. Ishii, N. Kobayashi, K. Hirose, N. Tsujii, and T. Mori, *Jpn. J. Appl. Phys.* **61**, SL1013 (2022).

Fig. 1. Bird's eye views of (a) the CoSb_3 (symmetric) thin film, (b) the CoSb_3 (unusual) thin film, and (c) the CoSb_3 (unusual) thin film with the replacement of Co (1) - Co (2) indicated by the red arrow. Co and Sb are depicted in blue and green, respectively. Co atoms are numbered as "1" \sim "8". "Lower" and "Upper" indicate the sites of "1, 4, 6, and 7" and "2, 3, 5, and 8", respectively.

Fig. 2. Bird's eye views of the (a) nonmagnetic, (b) ferromagnetic, and (c) replacement of Sc (1) - Co (2) in Sc-doped CoSb_3 (unusual) thin films. Sc, Co, and Sb are depicted in pink, blue, and green, respectively.

Fig. 3. Bird's eye views of the (a) nonmagnetic, (b) ferromagnetic, and (c) replacement of Ti (1) - Co (2) in Ti-doped CoSb_3 (unusual) thin films. Ti, Co, and Sb are depicted in grey, blue, and green, respectively. The evidently different atomic positions between (a) and (b) are labeled by red numbers and those between (b) and (c) are labeled by red (1 and 6) and black numbers (11).

Fig. 4. Bird's eye views of the (a) nonmagnetic Sc-, (b) ferromagnetic Sc-, (c) non-magnetic Ti-, and (d) ferromagnetic Ti-doped CoSb_3 (symmetric) thin films. Sc, Ti, Co, and Sb are depicted in pink, grey, blue, and green, respectively.

Fig. 5. Magnetic moment of each atom in the V-doped CoSb_3 (unusual) thin film. V, Co, and Sb atoms are denoted by 1, 2-8, and 9-32 on the horizontal axis, respectively. The inset shows the bird's eye view of the V-doped CoSb_3 (unusual) thin film where V and Co atoms are numbered. V, Co, and Sb are depicted in red, blue and green, respectively.

Fig. 6. Magnetic moment of each atom in the Mn-doped CoSb_3 (unusual) thin film. Mn, Co, and Sb atoms are denoted by 1, 2-8, and 9-32 on the horizontal axis, respectively. The inset shows the bird's eye view of the Mn-doped CoSb_3 (unusual) thin film where Mn and Co atoms are numbered. Mn, Co, and Sb are depicted in magenta, blue and green, respectively.

Fig. 7. Magnetic moment of each atom in the Ti-doped CoSb_3 (unusual) thin film with the replacement. The Ti dopant is denoted by 2 on the horizontal axis. Co atoms are denoted by 1 and 3-8 on the horizontal axis. Sb atoms are denoted by 9-32 on the horizontal axis. The inset shows the bird's eye view of the Ti-doped CoSb_3 (unusual) thin film with the replacement where Ti and Co atoms are numbered. Ti, Co, and Sb are depicted in grey, blue and green, respectively.

Fig. 8. Total and partial DOSs (states/eV cell) of (a) nonmagnetic and (b) ferromagnetic Mn-doped CoSb_3 (symmetric) thin films. Total and partial DOSs (states/eV

cell) of (c) nonmagnetic and (d) ferromagnetic Mn-doped CoSb_3 (unusual) thin films. The DOS curves of Total, Mn, Co, and Sb are plotted by magenta, red, blue, and green, respectively. The vertical scale is “states/eV cell” and linear. The Fermi level (E_f) is indicated by “0” on the horizontal axis. The insets show the expanded DOS around the Fermi level.

Fig. 9. Total and partial DOSs (states/eV cell) of (a) ferromagnetic and (b) replacement of Sc (1) - Co (2) in Sc-doped CoSb_3 (unusual) thin films. The DOS curves of Total, Sc, Co, and Sb are plotted by magenta, red, blue, and green, respectively. The vertical scale is “states/eV cell” and linear. The Fermi level (E_f) is indicated by “0” on the horizontal axis.

Fig. 10. Total and partial DOSs (states/eV cell) of (a) ferromagnetic and (b) replacement of Ti (1) - Co (2) in Ti-doped CoSb_3 (unusual) thin films. The DOS curves of Total, Ti, Co, and Sb are plotted by magenta, red, blue, and green, respectively. The vertical scale is “states/eV cell” and linear. The Fermi level (E_f) is indicated by “0” on the horizontal axis.

Table I. Total energy differences, average atomic position differences, and total magnetic moments. Thin films, cutoff energy [Ry] (Cutoff), number of k -points (N_k), number of atoms (N_a) in the supercell, magnetic states (“MS”; NM: Nonmagnetic, FM: Ferromagnetic), total energy differences per the supercell (= cell) (eV/cell) as $\Delta E_{\text{FM-NM}}$, average atomic position differences per atom (\AA) between the nonmagnetic and ferromagnetic cases as $\Delta D_{\text{FM-NM}}$, and total magnetic moment values (μ_B) as “Total”. Negative (positive) values of $\Delta E_{\text{FM-NM}}$ indicate more stable (more unstable).

Thin film	Cutoff	N_k	N_a	MS	$\Delta E_{\text{FM-NM}}$	$\Delta D_{\text{FM-NM}}$	Total (μ_B)
CoSb ₃ (symmetric) ¹⁰⁾	81	16	36	NM	0.0	-	-
CoSb ₃ (symmetric) ¹⁰⁾	81	16	36	FM	0.001	0.002	0.033
Sc-doped CoSb ₃ (symmetric)	81	16	36	NM	0.0	-	-
Sc-doped CoSb ₃ (symmetric)	81	16	36	FM	-0.03	0.120	0.021
Ti-doped CoSb ₃ (symmetric)	81	16	36	NM	0.0	-	-
Ti-doped CoSb ₃ (symmetric)	81	16	36	FM	0.005	0.006	0.042
V-doped CoSb ₃ (symmetric)	81	16	36	NM	0.0	-	-
V-doped CoSb ₃ (symmetric)	81	16	36	FM	-0.35	0.028	2.000
Cr-doped CoSb ₃ (symmetric) ¹⁰⁾	81	16	36	NM	0.0	-	-
Cr-doped CoSb ₃ (symmetric) ¹⁰⁾	81	16	36	FM	-0.52	0.049	2.940
Mn-doped CoSb ₃ (symmetric)	81	16	36	NM	0.0	-	-
Mn-doped CoSb ₃ (symmetric)	81	16	36	FM	-0.27	0.042	2.449
CoSb ₃ (unusual) ¹⁰⁾	81	16	32	NM	0.0	-	-
CoSb ₃ (unusual) ¹⁰⁾	81	16	32	FM	-2.40	0.205	8.291
Sc-doped CoSb ₃ (unusual)	81	16	32	NM	0.0	-	-
Sc-doped CoSb ₃ (unusual)	81	16	32	FM	3.61	1.168	8.485
Ti-doped CoSb ₃ (unusual)	81	16	32	NM	0.0	-	-
Ti-doped CoSb ₃ (unusual)	81	16	32	FM	-1.87	0.571	8.639
V-doped CoSb ₃ (unusual)	81	16	32	NM	0.0	-	-
V-doped CoSb ₃ (unusual)	81	16	32	FM	-1.94	0.511	10.001
Cr-doped CoSb ₃ (unusual) ¹⁰⁾	81	16	32	NM	0.0	-	-
Cr-doped CoSb ₃ (unusual) ¹⁰⁾	81	16	32	FM	-2.04	0.442	11.100
Mn-doped CoSb ₃ (unusual)	81	16	32	NM	0.0	-	-
Mn-doped CoSb ₃ (unusual)	81	16	32	FM	-1.80	0.448	11.655

Table II. Total magnetic moments and magnetic moments of dopants. Thin films, total magnetic moment values (μ_B) of thin films as “Total”, magnetic moment values (μ_B/atom) of dopants as “Dopant”, and magnetic moment values (μ_B/atom) of replaced Co atoms as “Replaced Co atom”.

Thin film	Total	Dopant	Replaced Co atom
CoSb ₃ (symmetric) ¹⁰⁾	0.033	-	-
Sc-doped CoSb ₃ (symmetric)	0.021	0.0006	-
Ti-doped CoSb ₃ (symmetric)	0.042	-0.041	-
V-doped CoSb ₃ (symmetric)	2.000	2.163	-
Cr-doped CoSb ₃ (symmetric) ¹⁰⁾	2.940	3.071	-
Mn-doped CoSb ₃ (symmetric)	2.449	3.005	-
CoSb ₃ (unusual) ¹⁰⁾	8.291	-	-
Sc-doped CoSb ₃ (unusual)	8.485	0.006	-
Ti-doped CoSb ₃ (unusual)	8.639	0.102	-
V-doped CoSb ₃ (unusual)	10.001	1.970	-
Cr-doped CoSb ₃ (unusual) ¹⁰⁾	11.100	3.328	-
Mn-doped CoSb ₃ (unusual)	11.655	3.601	-
Sc-Co replaced (unusual, nonrelaxed)	6.704	-0.090	2.179
Sc-Co replaced (unusual, relaxed)	5.711	-0.059	0.097
Ti-Co replaced (unusual, nonrelaxed)	5.015	-1.636	1.424
Ti-Co replaced (unusual, relaxed)	3.685	-1.969	0.133

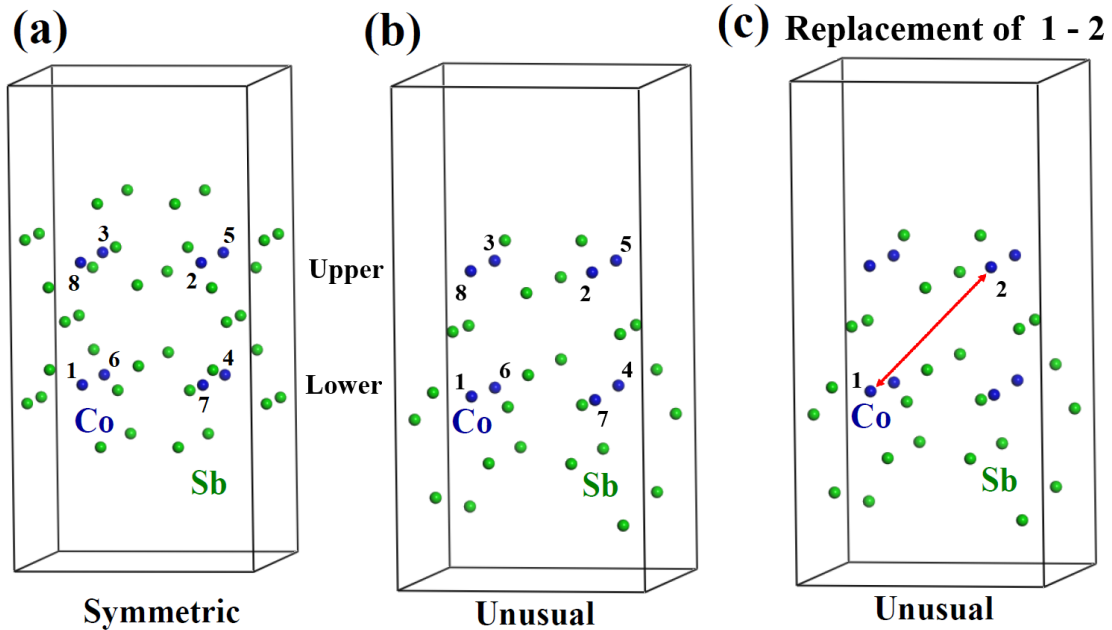


Fig. 1. Bird's eye views of (a) the CoSb₃ (symmetric) thin film, (b) the CoSb₃ (unusual) thin film, and (c) the CoSb₃ (unusual) thin film with the replacement of Co (1) - Co (2) indicated by the red arrow. Co and Sb are depicted in blue and green, respectively. Co atoms are numbered as “1” ~ “8”. “Lower” and “Upper” indicate the sites of “1, 4, 6, and 7” and “2, 3, 5, and 8”, respectively.

Table III. Stoner’s criterion. Atom, exchange parameters (I , eV), density of states per spin at the Fermi level ($D(E_f)$, states/eV atom spin), the values of $ID(E_f)$, “SC”, and “calc.”. “SC” indicates whether Stoner’s criterion is satisfied (ferromagnetic, FM) or not satisfied (nonmagnetic, NM). “calc.” indicates the calculated magnetic moment (μ_B /atom) of bulk and dopants. “(FM)” indicates the ferromagnetic behavior where the calculated magnetic moment is greater than 0.7.

Atom	I (eV)	$D(E_f)$	$ID(E_f)$	SC	calc.
Co(fcc) ¹⁰⁾	0.9792	0.9	0.9	NM	1.97 (FM)
Co(hcp) ¹⁰⁾	0.9792	1.2	1.2	FM	1.88 (FM)
Sc(bcc)	0.68	1.2	0.8	NM	0.72 (FM)
Sc(fcc)	0.68	1.0	0.7	NM	-
Sc(hcp)	0.68	1.0	0.7	NM	-
Ti(hcp)	0.68	0.5	0.3	NM	-
V(bcc)	0.7072	0.9	0.6	NM	0.0003
Cr(bcc) ¹⁰⁾	0.7616	0.7	0.5	NM	-
Mn(fcc)	0.816	0.7	0.6	NM	-
Doped Sc atom (symmetric)	0.68	0.2	0.1	NM	0.0006
Doped Ti atom (symmetric)	0.68	0.6	0.4	NM	-0.041
Doped V atom (symmetric)	0.7072	1.3	0.9	NM	2.163 (FM)
Doped Cr atom (symmetric) ¹⁰⁾	0.7616	1.2	0.9	NM	3.071 (FM)
Doped Mn atom (symmetric)	0.816	0.6	0.5	NM	3.005 (FM)
Doped Sc atom (unusual)	0.68	0.2	0.1	NM	0.006
Doped Ti atom (unusual)	0.68	1.0	0.7	NM	0.102
Doped V atom (unusual)	0.7072	1.5	1.1	FM	1.970 (FM)
Doped Cr atom (unusual) ¹⁰⁾	0.7616	1.2	0.9	NM	3.328 (FM)
Doped Mn atom (unusual)	0.816	1.0	0.8	NM	3.601 (FM)

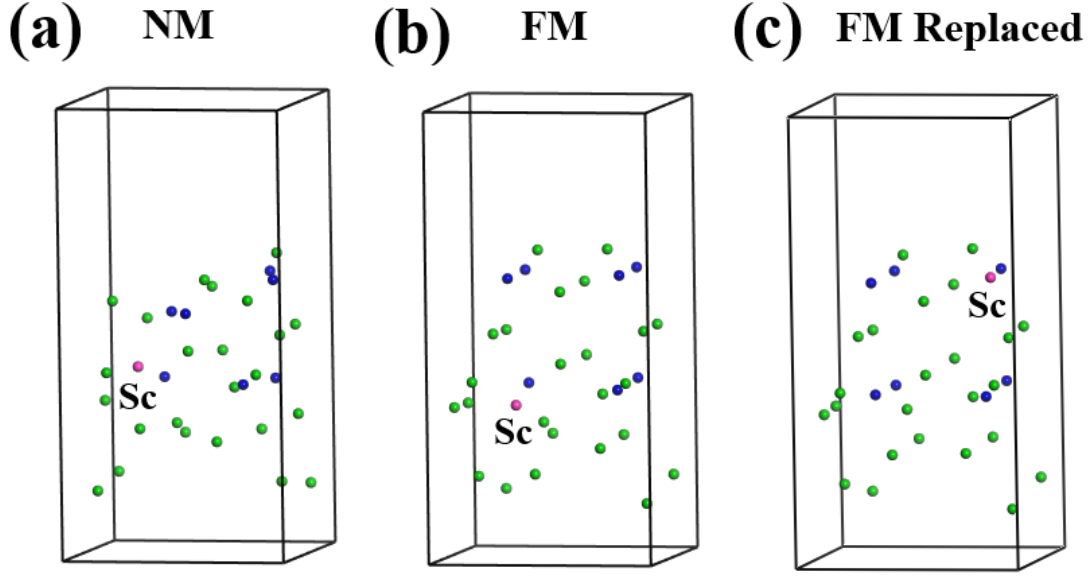


Fig. 2. Bird's eye views of the (a) nonmagnetic, (b) ferromagnetic, and (c) replacement of Sc (1) - Co (2) in Sc-doped CoSb_3 (unusual) thin films. Sc, Co, and Sb are depicted in pink, blue, and green, respectively.

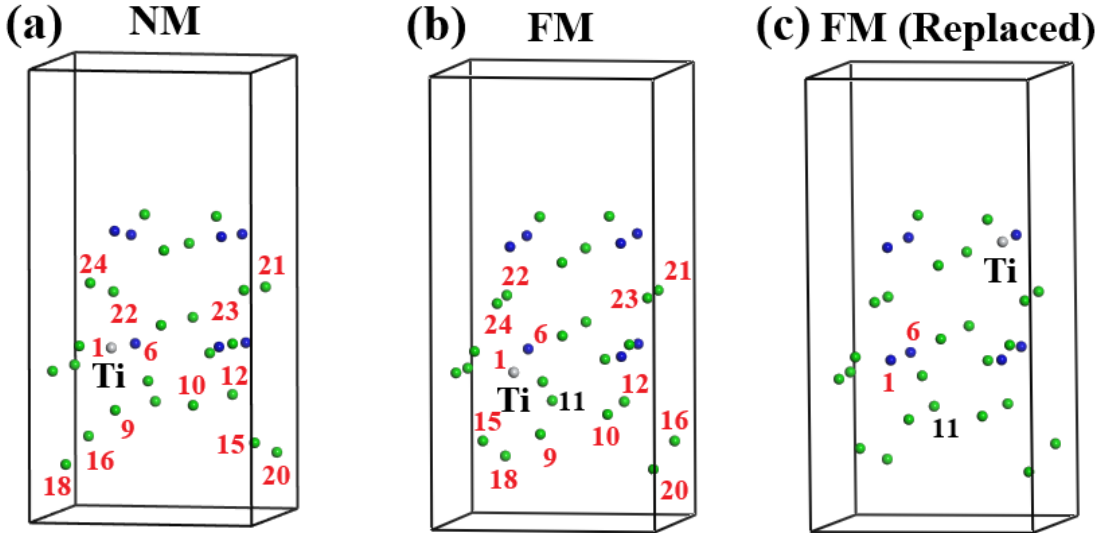


Fig. 3. Bird's eye views of the (a) nonmagnetic, (b) ferromagnetic, and (c) replacement of Ti (1) - Co (2) in Ti-doped CoSb_3 (unusual) thin films. Ti, Co, and Sb are depicted in grey, blue, and green, respectively. The evidently different atomic positions between (a) and (b) are labeled by red numbers and those between (b) and (c) are labeled by red (1 and 6) and black numbers (11).

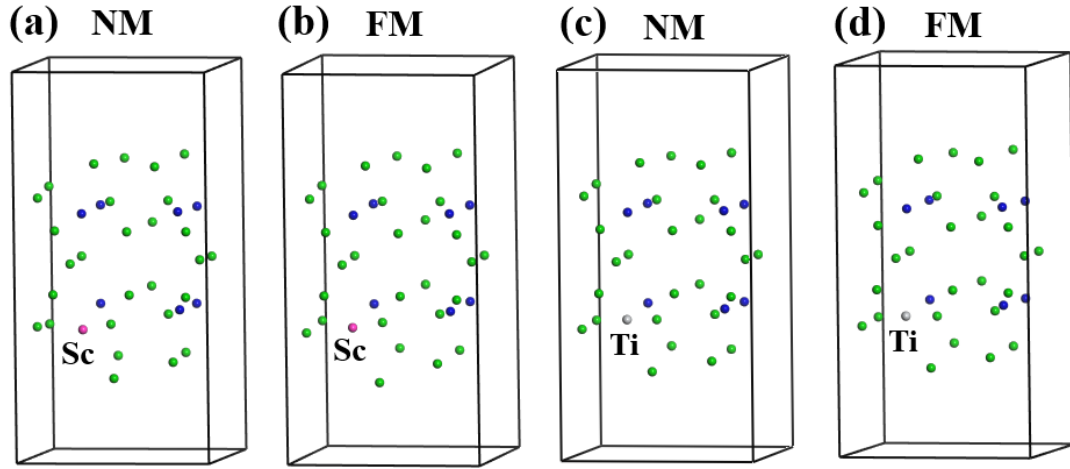


Fig. 4. Bird's eye views of the (a) nonmagnetic Sc-, (b) ferromagnetic Sc-, (c) nonmagnetic Ti-, and (d) ferromagnetic Ti-doped CoSb_3 (symmetric) thin films. Sc, Ti, Co, and Sb are depicted in pink, grey, blue, and green, respectively.

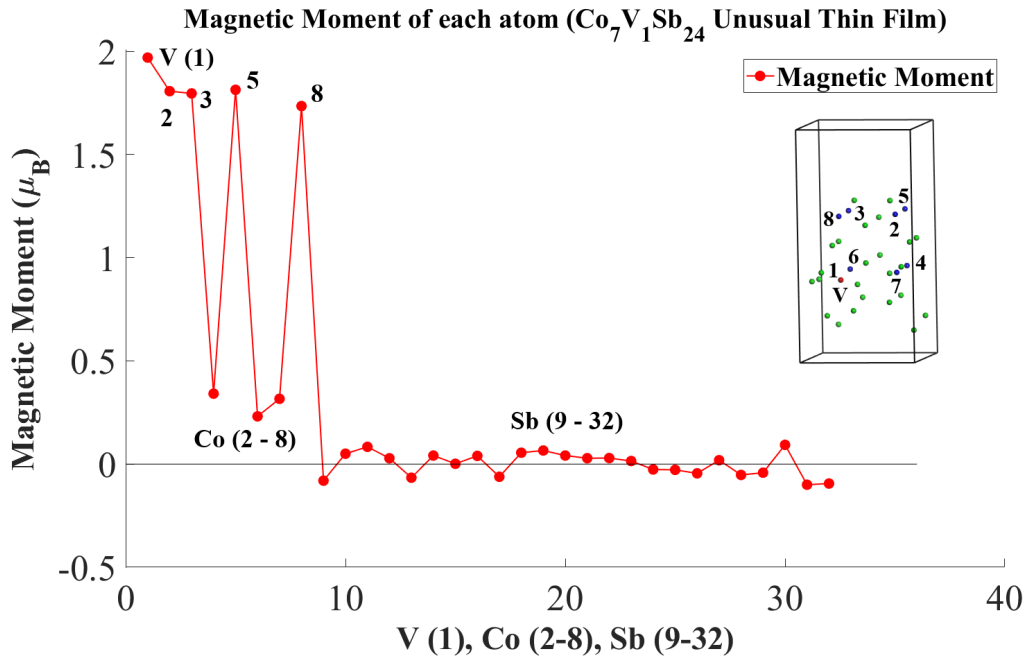


Fig. 5. Magnetic moment of each atom in the V-doped CoSb_3 (unusual) thin film. V, Co, and Sb atoms are denoted by 1, 2-8, and 9-32 on the horizontal axis, respectively. The inset shows the bird's eye view of the V-doped CoSb_3 (unusual) thin film where V and Co atoms are numbered. V, Co, and Sb are depicted in red, blue and green, respectively.

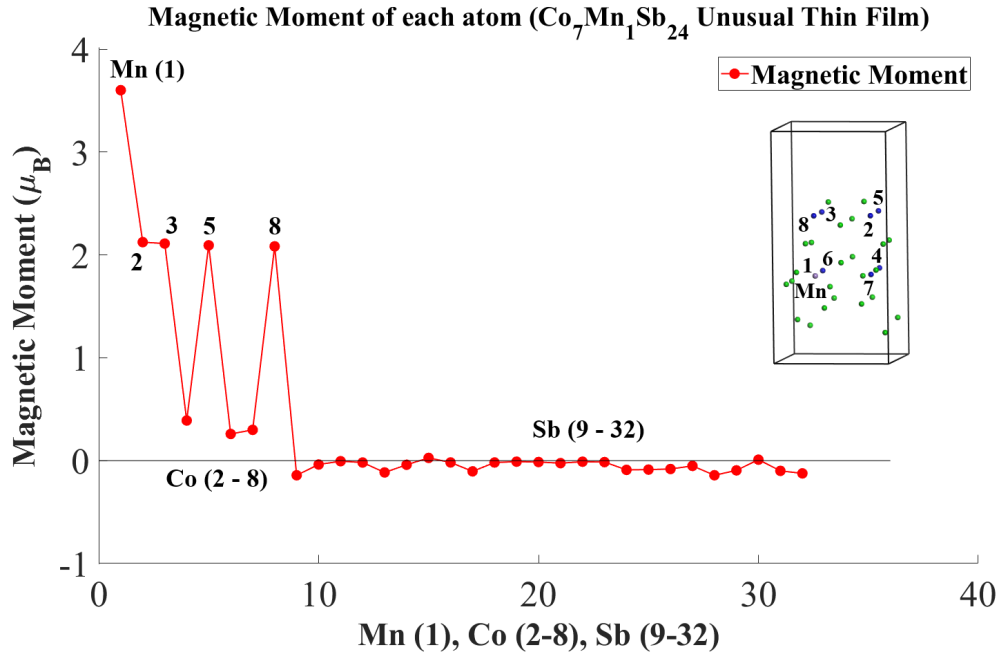


Fig. 6. Magnetic moment of each atom in the Mn-doped CoSb_3 (unusual) thin film. Mn, Co, and Sb atoms are denoted by 1, 2-8, and 9-32 on the horizontal axis, respectively. The inset shows the bird's eye view of the Mn-doped CoSb_3 (unusual) thin film where Mn and Co atoms are numbered. Mn, Co, and Sb are depicted in magenta, blue and green, respectively.

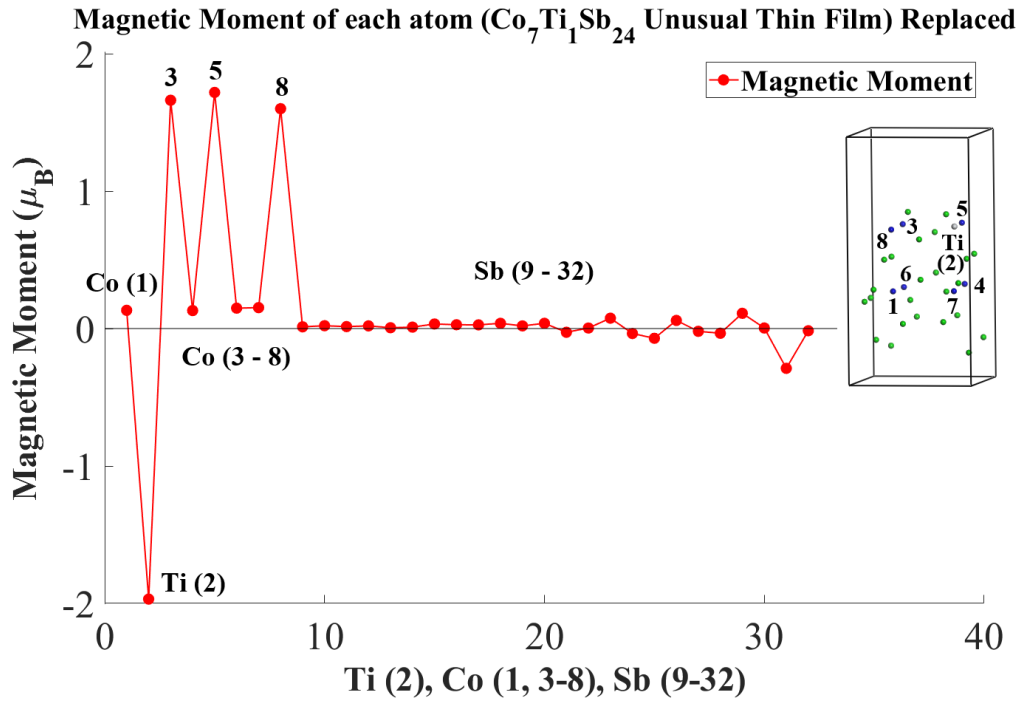


Fig. 7. Magnetic moment of each atom in the Ti-doped CoSb_3 (unusual) thin film with the replacement. The Ti dopant is denoted by 2 on the horizontal axis. Co atoms are denoted by 1 and 3-8 on the horizontal axis. Sb atoms are denoted by 9-32 on the horizontal axis. The inset shows the bird's eye view of the Ti-doped CoSb_3 (unusual) thin film with the replacement where Ti and Co atoms are numbered. Ti, Co, and Sb are depicted in grey, blue and green, respectively.

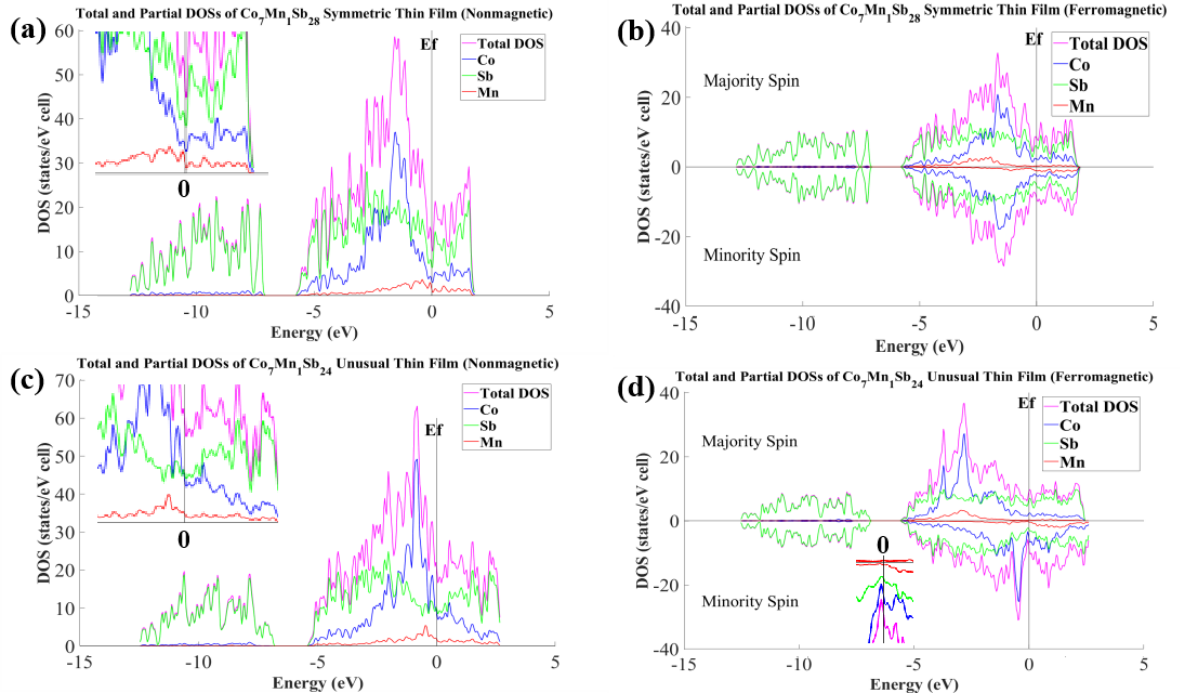


Fig. 8. Total and partial DOSs (states/eV cell) of (a) nonmagnetic and (b) ferromagnetic Mn-doped CoSb_3 (symmetric) thin films. Total and partial DOSs (states/eV cell) of (c) nonmagnetic and (d) ferromagnetic Mn-doped CoSb_3 (unusual) thin films. The DOS curves of Total, Mn, Co, and Sb are plotted by magenta, red, blue, and green, respectively. The vertical scale is “states/eV cell” and linear. The Fermi level (E_f) is indicated by “0” on the horizontal axis. The insets show the expanded DOS around the Fermi level.

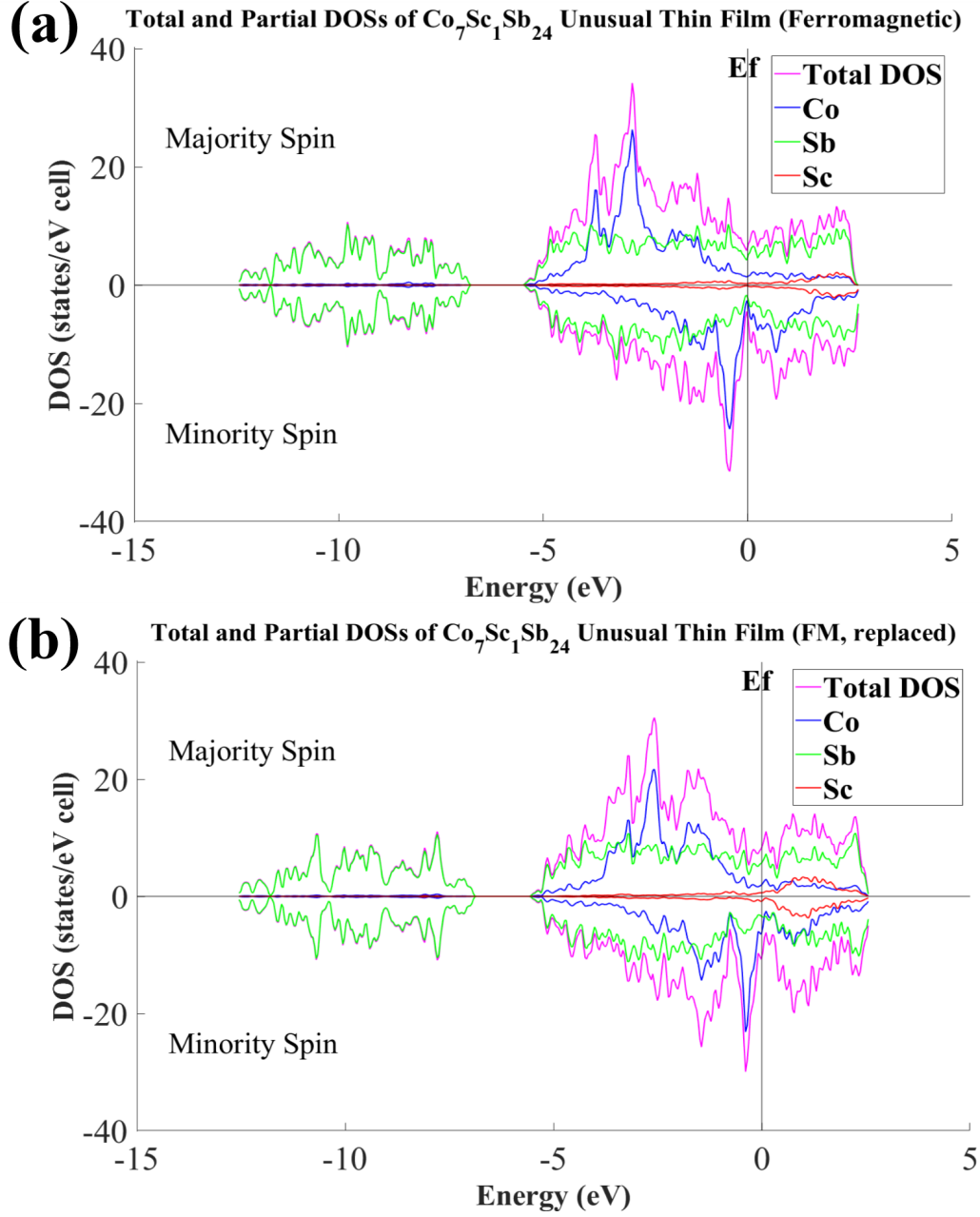


Fig. 9. Total and partial DOSs (states/eV cell) of (a) ferromagnetic and (b) replacement of Sc (1) - Co (2) in Sc-doped CoSb_3 (unusual) thin films. The DOS curves of Total, Sc, Co, and Sb are plotted by magenta, red, blue, and green, respectively. The vertical scale is “states/eV cell” and linear. The Fermi level (E_f) is indicated by “0” on the horizontal axis.

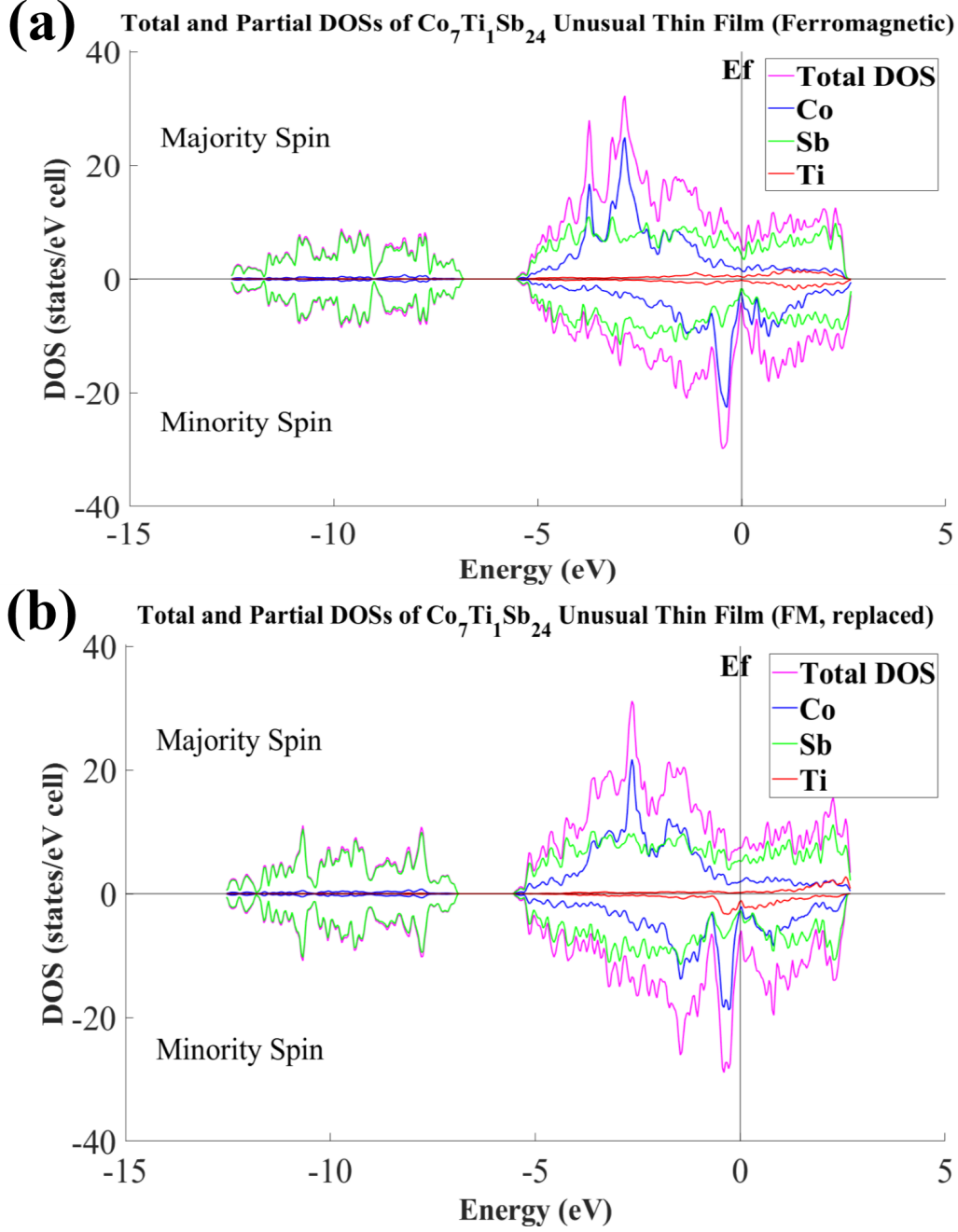


Fig. 10. Total and partial DOSs (states/eV cell) of (a) ferromagnetic, and (b) replacement of Ti (1) - Co (2) in Ti-doped CoSb_3 (unusual) thin films. The DOS curves of Total, Ti, Co, and Sb are plotted by magenta, red, blue, and green, respectively. The vertical scale is “states/eV cell” and linear. The Fermi level (E_f) is indicated by “0” on the horizontal axis.